Low-Loss Frequency-Agile Bandpass Filters With Controllable Bandwidth and Suppressed Second Harmonic

Xiu Yin Zhang, *Member, IEEE*, Quan Xue, *Senior Member, IEEE*, Chi Hou Chan, *Fellow, IEEE*, and Bin-Jie Hu, *Member, IEEE*

***Abstract*—This paper presents a novel approach to design frequency-agile bandpass filters with constant absolute bandwidth and passband shape, as well as a suppressed second harmonic. A novel mixed electric and magnetic coupling scheme is proposed to control the coupling coefficient variation. Theoretical analysis indicates that it is able to achieve desired coupling coefficients between the proposed resonators at various frequencies so as to obtain constant absolute bandwidth. Moreover, this half- wavelength resonator has a Q higher than the quarter- and half- wavelength counterparts, thus resulting in low insertion loss. A filter of this type is designed to validate the proposed idea. To remove the spurious responses of the filter, a method is then introduced to suppress the second harmonic without degrading the passband performance. For demonstration, two frequency-agile filters with 60- and 80-MHz constant absolute bandwidth are implemented with the frequency tuning range from 680 to 1000 MHz. Comparisons of experimental and simulated results are presented to verify the theoretical predications.**

***Index Terms*—Bandpass filter, constant bandwidth, harmonic suppression, Q factor, tunable filter.**

I. Introduction

FREQUENCY-AGILE bandpass filters are essential for multiband and wideband systems. Extensive research has been done and different tuning devices have been employed. Semiconductor varactors are widely used due to the high tuning speed and reliability [1]–[11]. Unfortunately, the Q of varactor diodes is usually low, leading to high insertion loss. In contrast, microelectromechanical system (MEMS) varactors possess higher Q and linearity [12], [13]; these, however, are expensive. Ferroelectric components have recently attracted much attention in tunable filter designs due to the tuablity of the dielectric constant [14]–[16].

Regardless of the tuning devices used, it is desirable in certain applications to maintain constant absolute bandwidth and passband shape as the passband is tuned. Various methods have been utilized to achieve constant absolute bandwidth. Hunter and Rhodes [1] used combline filter topology realized in a suspended substrate stripline with the resonator's electrical length of 53° to obtain constant absolute bandwidth. This method can also be used in microstrip combline filters using stepped-impedance resonators [3]. Another method to achieve constant absolute bandwidth is to introduce a fixed or variable attenuation pole near the passband to force nearly constant bandwidth [4], [17]. The inter-stage coupling variation can also be controlled to obtain constant absolute bandwidth. In [5], a variable capacitor is utilized to control the coupling. In [6], an independent electric and magnetic coupling scheme is used to manipulate the coupling coefficient variation so that the bandwidth can be controlled.

Insertion loss is another important issue in frequency-agile bandpass filter designs. For a filter with a specific bandwidth, the insertion loss is mainly determined by the resonator Q. In order to reduce the insertion loss, high-Q components, e.g., MEMS components, are necessitated [12], [13], thus leading to high cost.

In this paper, a novel approach is proposed to design frequency-agile bandpass filters with constant absolute bandwidth and passband shape together with suppressed second harmonic. The proposed resonator is composed of an open-ended transmission line with one varactor loaded at one end. The variation of the inter-stage coupling coefficient can be controlled by using a novel mixed electric and magnetic coupling scheme; this allows that the requirement of constant absolute bandwidth can be met. Moreover, this half-wavelength resonator has higher overall Q than the widely used quarter- and half-wavelength counterparts. In turn, low-cost silicon varactors can be used to obtain acceptable performance. Using the proposed resonators and coupling scheme, a frequency-agile bandpass filters with 80-MHz constant absolute bandwidth is demonstrated with the frequency tuning range from 680 to 1000 MHz. A method is then introduced to suppress the second harmonic without affecting the passband performance. Two tunable filters with 60- and 80-MHz constant absolute bandwidth and suppressed second harmonic are implemented. Experimental and simulated results are presented to verify the proposed method.

Manuscript received November 05, 2009, revised February 09, 2010; accepted February 13, 2010. Date of publication May 10, 2010; date of current version June 11, 2010. This work was supported by the Research Grants Council of Hong Kong Special Administrative Region, China, under Grant CityU 110808. This work was supported in part by the Fundamental Research Funds for the Central Universities, South China University of Technology (SCUT), under Grant 2009ZZ0066, by the National Key Project of Science and Technology of China under Grant 2009ZX03006-003, and by the National Natural Science Foundation of China (NSFC)–Natural Science Associated Foundation (NSAF) under Grant 10976010.

X. Y. Zhang and B.-J. Hu are with the School of Electronic and Information Engineering, South China University of Technology, Guangzhou 510640, China (e-mail: zhangxiuyin@scut.edu.cn; eebjiehu@scut.edu.cn).

Q. Xue and C. H. Chan are with the State Key Laboratory of Millimeter Waves, Department of Electronic Engineering, City University of Hong Kong, Kowloon, Hong Kong (e-mail: eeqxue@cityu.edu.hk; eechic@cityu.edu.hk).

Color versions of one or more of the figures in this paper are available online at http://ieeexplore.ieee.org.

Digital Object Identifier 10.1109/TMTT.2010.2048250

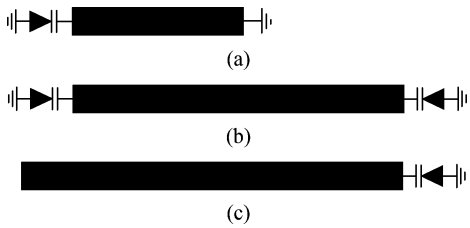

Fig. 1. (a) Conventional $\lambda/4$ resonator with one varactor. (b) Conventional $\lambda/2$ resonator with two varactors. (c) Proposed asymmetric $\lambda/2$ resonator with one varactor.

II. Design Theory

To design low-loss tunable bandpass filters with constant absolute bandwidth, the requirement on the unloaded resonator Q, coupling coefficients, and external Q should be satisfied.

A. Unloaded Resonator Q

It is common that tunable filter designs employ $\lambda/4$ and $\lambda/2$ resonators. Fig. 1(a) shows the configuration of a conventional $\lambda/4$ resonator. One end of the microstrip line is loaded by a varactor and the other end is shorted[2], [3], [6], [8]. Fig. 1(b) shows a conventional $\lambda/2$ resonator with two varactors loaded at the two ends, forming a symmetric structure with respect to the center plane of the transmission line [4], [10], [11]. These two types of resonators are widely used in tunable filter designs.

In this design, a novel $\lambda/2$ resonator is proposed, as shown in Fig. 1(c). Only one varactor is loaded at one end and the structure is asymmetric. The proposed resonator has higher Q than the other two counterparts. For comparative purposes, it is assumed that the Q values of all of the varactors are identical and lower than that of conventional microstrip line; the latter is true for most silicon varactors. The three resonators have the same fundamental resonant frequency under the same bias voltage. In this case, the microstrip line of the asymmetric $\lambda/2$ resonator is longer than the symmetric one. Since the microstrip has higher Q than the varactor, the overall Q of the proposed resonator is higher than that of the symmetric $\lambda/2$ resonator. On the other hand, the symmetric $\lambda/2$ resonator is equivalent to the $\lambda/4$ resonator at the fundamental resonant frequency. Hence, they have the same unloaded Q. As a result, the proposed resonator has higher unloaded Q than the others. For demonstration, a simulation study is conducted to extract the unloaded Q's. The same varactor model and microstrip lines are utilized in the simulation and the three resonators are tuned to resonate at the same frequency of 850 MHz. The resonators in Fig. 1(a)–(c) have the unloaded Q's of 58, 57, and 68, respectively. Hence, the proposed resonator has a Q higher than others. In turn, for given filter specifications, use of the proposed resonator can alleviate the requirement on the varactor Q, resulting in low-cost design.

B. Coupling Coefficient

For a second-order filter, the required coupling coefficient k is given by

$$k = \frac{\mathrm{BW}}{f_0\sqrt{g_1 g_2}} \tag{1}$$

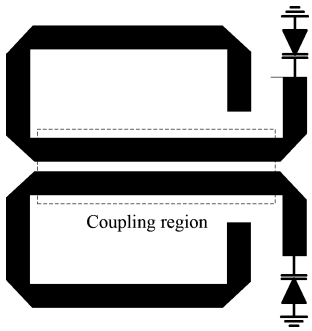

Fig. 2. Inter-stage coupling structure.

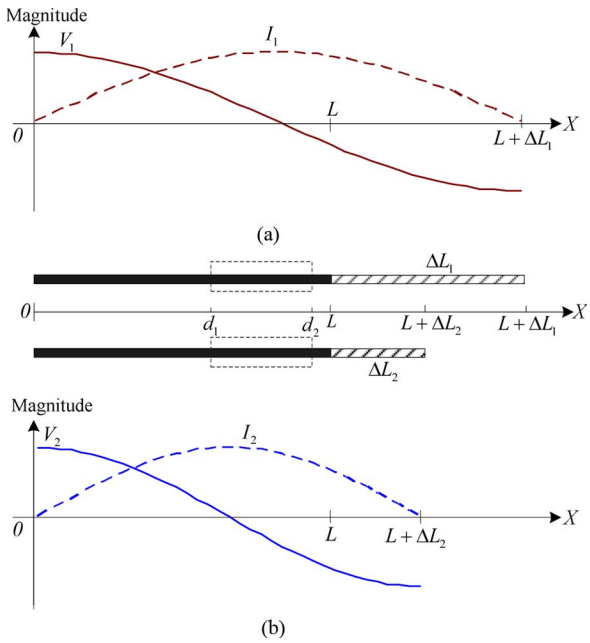

Fig. 3. Normalized voltage and current distributions on the resonator. (a) At lower frequency f_L. (b) At upper frequency f_U.

where BW represents the absolute bandwidth, g_1 and g_2 are the element values of the low-pass prototype filter, and f_0 is the center frequency. As can be seen, to achieve constant absolute bandwidth over the tuning range, the coupling coefficient should become lower as the center frequency increases.

To obtain the desired coupling coefficients, a novel mixed electric and magnetic coupling scheme is proposed, as shown in Fig. 2. For coupled microstrip lines, the electric and magnetic coupling can be evaluated by studying the voltage and current distributions [19]. Ignoring the parasitic effects, the varactor can be made equivalent to a segment of open-ended microstrip line. Fig. 3 shows the equivalent circuits of one resonator under different varactor bias voltages. The darkened parts denote real microstrip lines with the length of L. The filled parts (ΔL_1 and ΔL_2) are equivalent to the varactor under different bias voltages. The region between d_1 and d_2 represent the lines in the coupling region.

When the capacitance of the varactor is larger, the equivalent microstrip line is longer (ΔL_1) and the resonant frequency is

lower (f_L). At fundamental resonance, the normalized voltage and current can be expressed as

$$V_1(x) = \cos\beta_1 x \tag{2}$$
$$I_1(x) = \sin\beta_1 x \tag{3}$$

where β_1 is the propagation constant at f_L. The voltage and current distributions are illustrated in Fig. 3(a). In the case of smaller varactor capacitance, the equivalent microstrip line is shorter (ΔL_2) and the resonant frequency is higher (f_U). Similarly, the voltage and current can be given as

$$V_2(x) = \cos\beta_2 x \tag{4}$$
$$I_2(x) = \sin\beta_2 x \tag{5}$$

where β_2 is the propagation constant at f_U. The voltage and current distributions are shown in Fig. 3(b). The electric and magnetic coupling coefficients k_e and k_m in the two cases can be expressed as [19]

$$|k_{e,i}| = p \times \int_{d_1}^{d_2} |V_i(x)|^2 dx = p \times \int_{d_1}^{d_2} (\cos\beta_i x)^2 dx \tag{6}$$
$$|k_{m,i}| = p \times \int_{d_1}^{d_2} |I_i(x)|^2 dx = p \times \int_{d_1}^{d_2} (\sin\beta_i x)^2 dx \tag{7}$$

where p is a positive constant and $i = 1, 2$, corresponding to the lower and upper frequencies, respectively.

The overall coupling coefficient can vary inversely with frequency if a proper coupling region is selected. Since the electric and magnetic coupling coefficients are out of phase, when the magnetic coupling is dominant, the magnitude of coupling coefficient is

$$|k_i| = |k_{m,i}| - |k_{e,i}|. \tag{8}$$

When the magnetic coupling varies inversely with frequency while the electric coupling varies directly with frequency, the net coupling is proportional to frequency. Fig. 4 illustrates such a case. Inspecting (6) and (7), we can find that the coupling strength can be indicated by the area below the curve of $|V_i(x)|^2$ and $|I_i(x)|^2$ between d_1 and d_2. From Fig. 4(a), it is observed that the electric coupling coefficient at lower frequency (indicated by the area below the dark red line (in online version) with cross symbols between d_1 and d_2) is lower than that at upper frequency (indicated by the area under the blue line (in online version) with square symbols between d_1 and d_2), namely,

$$|k_{e,1}| < |k_{e,2}|. \tag{9}$$

Similarly, Fig. 4(b) indicates that

$$|k_{m,1}| > |k_{m,2}|. \tag{10}$$

Inspecting (8)–(10) gives

$$|k_1| > |k_2|. \tag{11}$$

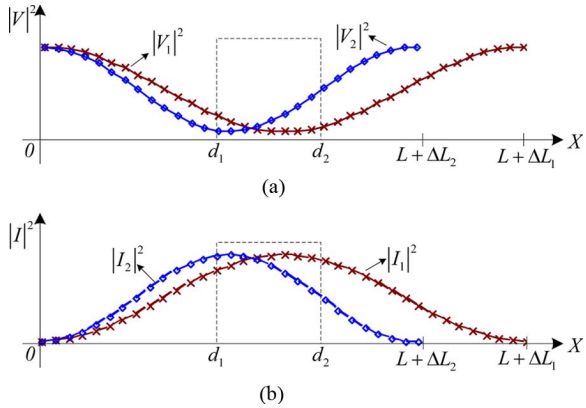

Fig. 4. Comparison of electric and magnetic coupling at various frequencies. (a) Electric coupling. (b) Magnetic coupling.

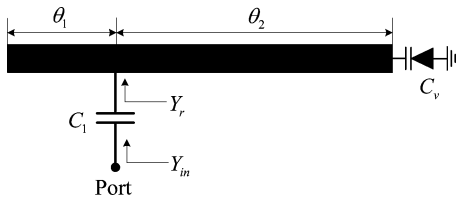

Fig. 5. Resonator with the input coupling network.

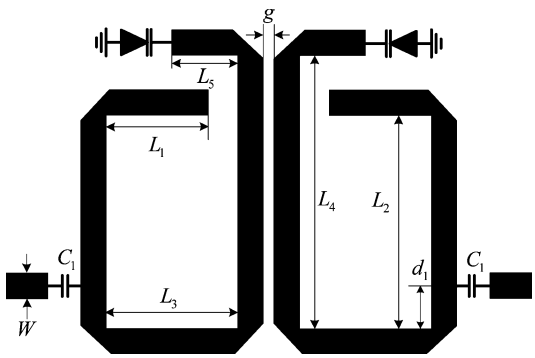

Fig. 6. Configuration of the tunable filter with constant absolute bandwidth.

Therefore, the coupling coefficient becomes lower as the center frequency is tuned upward; this can meet the requirement of constant absolute bandwidth.

C. External Q

The required external Q or Q_e for a second-order filter is given by

$$Q_e = \frac{f_0}{\mathrm{BW}\sqrt{g_0 g_1}}. \tag{12}$$

To maintain constant absolute bandwidth, Q_e should increase as the frequency shifts upward. This can be realized by using the structure shown in Fig. 5.

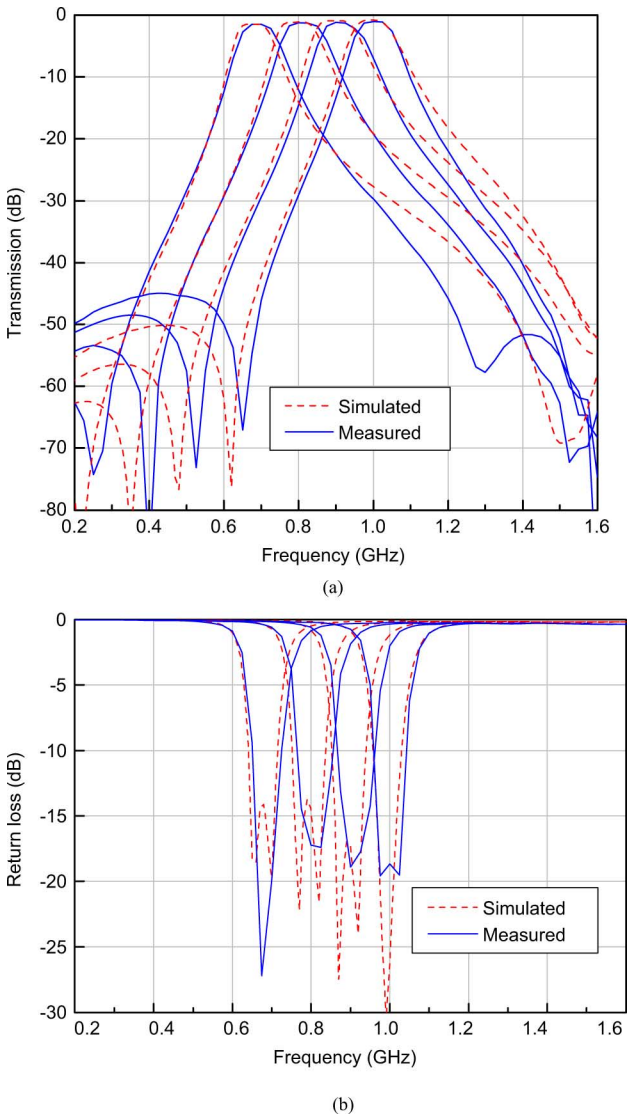

Fig. 7. Simulated and measured responses. (a) Transmission. (b) Return loss.

To facilitate the analysis, the parasitic effects of the varactor and the line discontinuity are ignored. The input admittance of the resonator Y_r, seen from the input port, is

$$Y_r = \frac{jY}{Y - \omega C_v \tan\theta_2}[Y(\tan\theta_1 + \tan\theta_2) + \omega C_v(1 - \tan\theta_1 \tan\theta_2)] \quad (13)$$

where Y is the characteristic admittance of the microstrip line, θ_1 and θ_2 are the electric length, and C_v is the capacitance of the varactor. The overall input admittance Y_{in} is

$$Y_{\text{in}} = \frac{j\omega C_1 Y_r}{j\omega C_1 + Y_r}. \quad (14)$$

Q_e is then determined as

$$Q_e = \frac{\omega_0}{2Y_0} \frac{\partial \text{Im}[Y_{\text{in}}]}{\partial \omega}\bigg|_{\omega=\omega_0}. \quad (15)$$

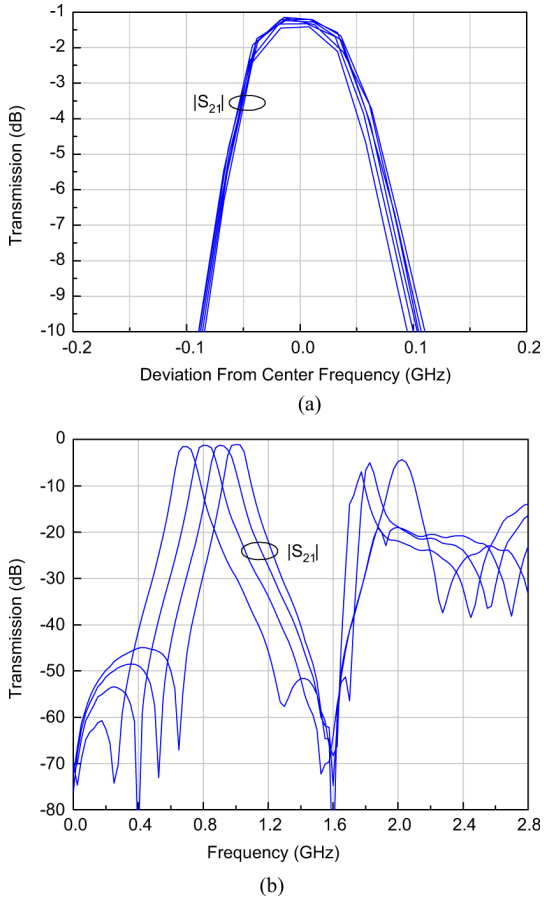

Fig. 8. Measured responses. (a) Superposition of the passband responses. (b) Wideband responses.

TABLE I
COMPARISON WITH OTHER DESIGN

	Resonator	Varactor Q	Loss tangent	Unloaded Q
[6]	λ/4 with one varactor	Around 2000	0.0009	53-152
This work	λ/2 with one varactor	35-100	0.0018	42-72

It can be seen that the capacitance C_1 and the electrical length θ_1 and θ_2 will affect Q_e. By properly choosing these three parameters, the desired Q_e can be obtained within the frequency tuning range.

III. FREQUENCY-AGILE FILTER IMPLEMENTATION

Based on the previous design theory, a frequency-agile filter with constant absolute bandwidth is implemented. The filter configuration is shown in Fig. 6. This filter employs two resonators. The silicon varactors are 1sv277 from Toshiba, Tokyo, Japan. The input and output feeding lines are tapped at the resonators through the capacitors. The tap position d_1 and the capacitance C_1 are tuned so as to fulfill the requirement of Q_e over the frequency tuning range.

The filter is fabricated on the substrate with the thickness of 0.82 mm, relative dielectric constant of 6.03, and loss tangent of 0.0018. The dimensions are determined as follows: $L_1 = 5.0$ mm, $L_2 = 18.8$ mm, $L_3 = 6.8$ mm, $L_4 = 22.0$ mm,

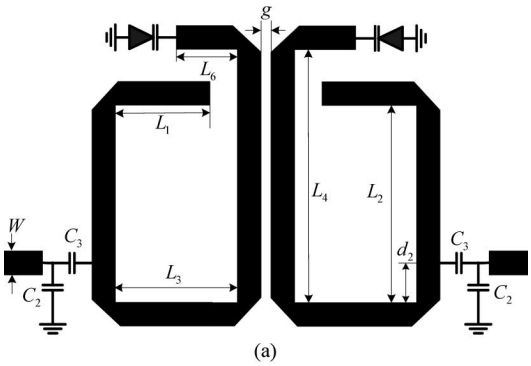

(a)

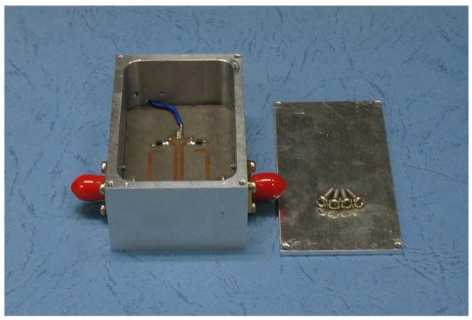

(a)

Fig. 9. Tunable filter with the suppressed second harmonic responses. (a) Filter configuration. (b) Photograph of the fabricated filter.

$L_5 = 3.5$ mm, $W = 1.2$ mm, $d_1 = 2.5$ mm, $g = 0.5$ mm, and $C_1 = 3$ pF. The filter is enclosed in a metal cavity with the dimensions of $5 \times 3.4 \times 2$ cm^3.

Fig. 7 shows the simulated and measured responses, which agree reasonably well with each other. As shown in Fig. 7(b), the center frequency can be tuned between 680 and 1000 MHz, featuring the fractional tuning range of 38%. The measured return loss over the tuning range is greater than 15 dB. For each tuning state, there are two transmission zeros near the passband edges, which improve the roll-off rate. These transmission zeros are due to the tap connections of input and output port, which lead to quarter-wavelength resonance. Fig. 8(a) shows a superposition of the measured passband responses at various frequencies. As can be observed, the passband shape and absolute bandwidth are kept nearly constant over the tuning range. The measured 1-dB absolute bandwidth is 80 ± 3.5 MHz. The variation is less than 4.4%, which is lower than those (7%–10%) in [1] and [6] and a little bit higher than those (3%–3.5%) in [3] and [4]. Therefore, the bandwidth can be considered as constant. For all the tuning states, the insertion loss is from 1.1 to 1.5 dB, thus indicating low insertion loss. The variation of insertion-loss in absolute value is 4.6%, which is lower than the value of 7.2% in [5] and 11.4% in [6].

This design is compared with that in [6], as tabulated in Table I. The measured unloaded Q of this filter is 42–72 from 680 to 1000 MHz. This is somewhat lower than the reported one of 53–152 from 850 to 1400 MHz in [6]. However, the design in [6] employed high-Q GaAs varactors and low-loss substrate. In contrast, this is a low-cost design, which utilizes ordinary silicon varactors and substrate. This indicates the superiority of the proposed resonator.

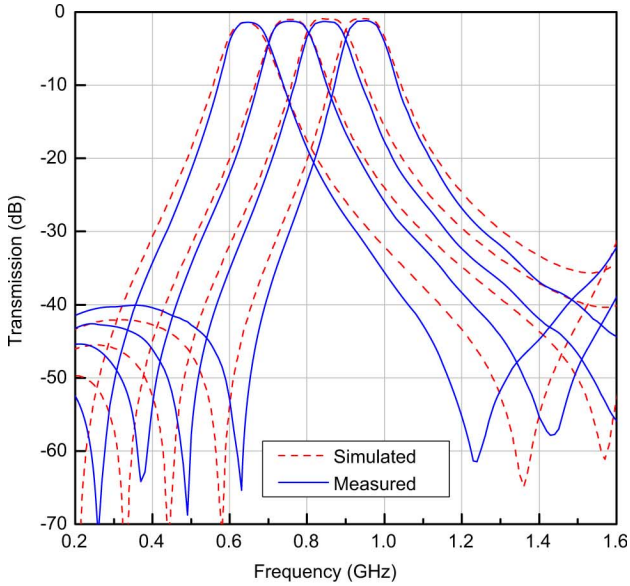

(a)

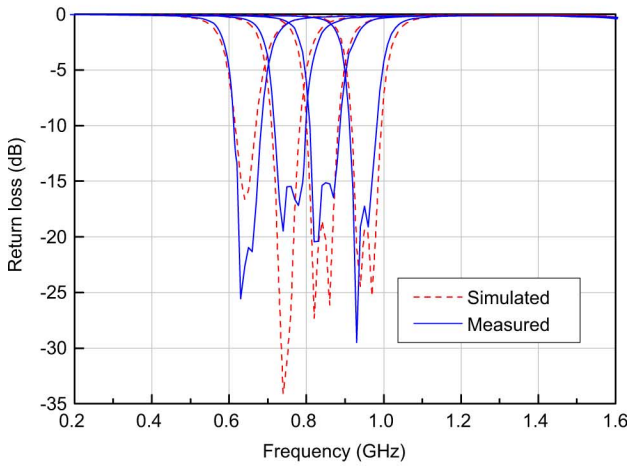

(b)

Fig. 10. Responses of the filter with 80-MHz bandwidth. (a) Transmission. (b) Return loss.

Despite the good passband performance of the implemented filter, it suffers from high second harmonic levels, as shown in Fig. 8(b). It is straightforward to suppress them using a low-pass or bandstop structure. However, it will induce extra insertion loss and increase the circuit size. In applications, it is desirable to reduce the harmonic levels without affecting the passband performance. This leads to the following designs.

IV. Frequency-Agile Filter With Suppressed Harmonic

The second harmonic of the previous filter can be suppressed by using input and output coupling networks with the intrinsic bandpass characteristic. Fig. 9 shows such a filter configuration. This filter is the same as the previous one aside from the input and output coupling networks. The shunt capacitor C_2 and series capacitor C_3 form a bandpass network. When the second harmonic is within the stopband of this bandpass network, they can be suppressed. On the other hand, the coupling networks affect Q_e. Based on (14), the input admittance can be derived as

$$Y'_{\text{in}} = \frac{j\omega Y_r(C_2 + C_3) - \omega^2 C_2 C_3}{j\omega C_3 + Y_r}. \tag{16}$$

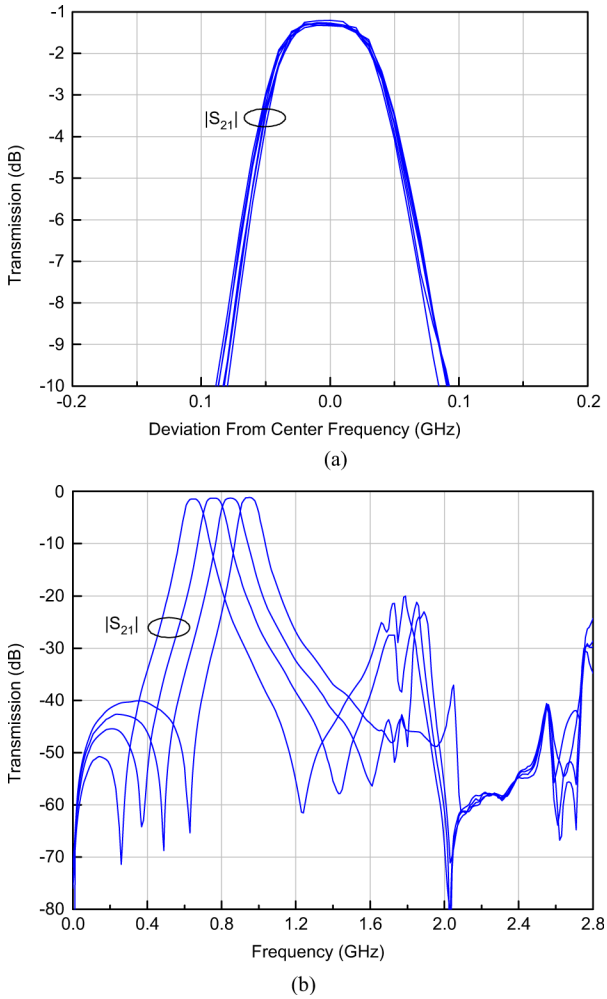

Fig. 11. Measured responses of the filter with 80-MHz bandwidth. (a) Superposition of the passband responses. (b) Wideband responses.

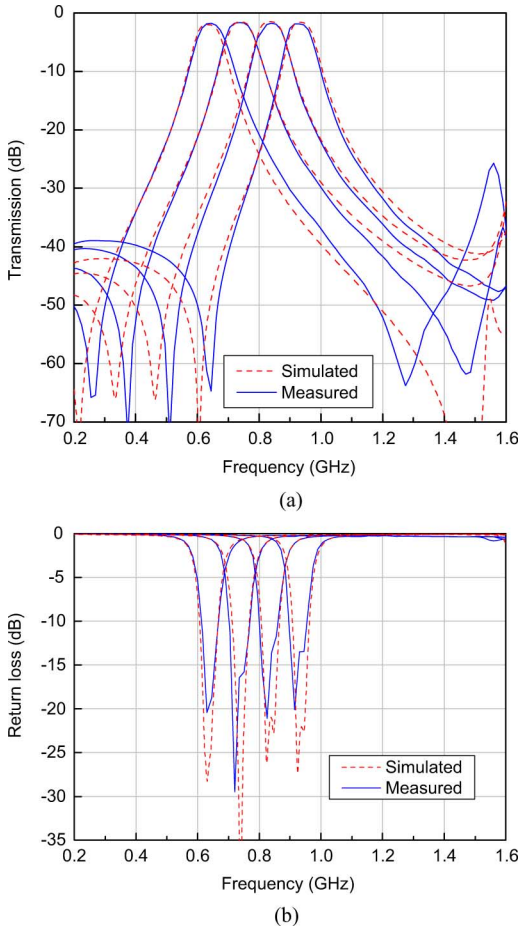

Fig. 12. Responses of the filter with 60-MHz bandwidth. (a) Transmission. (b) Return loss.

Inspecting (15) and (16), we can find that the two capacitors will affect Q_e. Therefore, the capacitors C_2 and C_3 should fulfill the requirements of both Q_e and harmonic suppression. It is noted that Q_e is controlled not only by the capacitance C_2 and C_3, but also by the tap position d_2. Hence, there are sufficient degrees of freedom to meet the requirements of both Q_e and harmonic suppression. In this manner, the harmonic can be suppressed without degrading passband performance.

Using the configuration, two filters with 80- and 60-MHz absolute bandwith are implemented with the suppressed second harmonic. The two filters are fabricated on the substrate with the relative dielectric constant of 6.03, thickness of 0.82 mm, and loss tangent of 0.0018. The filter with 80-MHz bandwidth has the following dimensions: $L_1 = 5.0$ mm, $L_2 = 18.8$ mm, $L_3 = 6.8$ mm, $L_4 = 22.0$ mm, $L_6 = 5.0$ mm, $W = 1.2$ mm, $d_2 = 2.8$ mm, $g = 0.5$ mm, $C_2 = 3.3$ pF, and $C_3 = 6.8$ pF. The overall size is around $0.12\,\lambda_g \times 0.12\,\lambda_g$, where λ_g is the guided wavelength at lowest passband frequency. The filter is enclosed in a metal cavity with the dimensions of $5 \times 3.4 \times 2$ cm^3. The fabricated filter is shown in Fig. 9(b).

Fig. 10 illustrates the simulated and measured results. The passband tuning range is from 650 to 960 MHz, featuring a 38% fractional tuning range. The measured in-band return loss is greater than 15 dB for all the tuning states. The measured 1-dB absolute bandwidth is 80 ± 3.5 MHz. The passband shape and insertion loss are maintained nearly constant over the tuning range, as shown in Fig. 11(a). The insertion loss ranges from 1.2 to 1.5 dB, which is nearly the same as the previous one; this indicates that the passband performance is nearly not affected. Fig. 11(b) shows the measured wideband responses. It can be seen that the second harmonic levels are below -20 dB. Hence, it can be summarized that the passband performance is preserved, while the second harmonic is suppressed. The input third-order intermodulation intercept point (IIP3) is measured at 2.5-V bias with 1-MHz frequency spacing. The IIP3 is measured at 13 dBm.

To demonstrate the wide applicability of this method, a filter with 60-MHz bandwidth is also implemented. The dimensions are as follows: $L_1 = 3.5$ mm, $L_2 = 16.8$ mm, $L_3 = 6.8$ mm, $L_4 = 20$ mm, $L_6 = 5.0$ mm, $W = 1.2$ mm, $d_2 = 3.5$ mm, $g = 0.55$ mm, $C_2 = 5$ pF, and $C_3 = 8$ pF. The filter is also enclosed in a metal cavity with the dimensions of $5 \times 3.4 \times 2$ cm^3. Fig. 12 shows the simulated and measured results. The passband frequency can be tuned from 630 to 930 MHz, featuring the fractional tuning range of 38.5%. The measured in-band return loss is around 20 dB for all the tuning states. The 1-dB absolute bandwidth is 60 ± 3 MHz. The passband shape and insertion loss are maintained nearly constant over the tuning

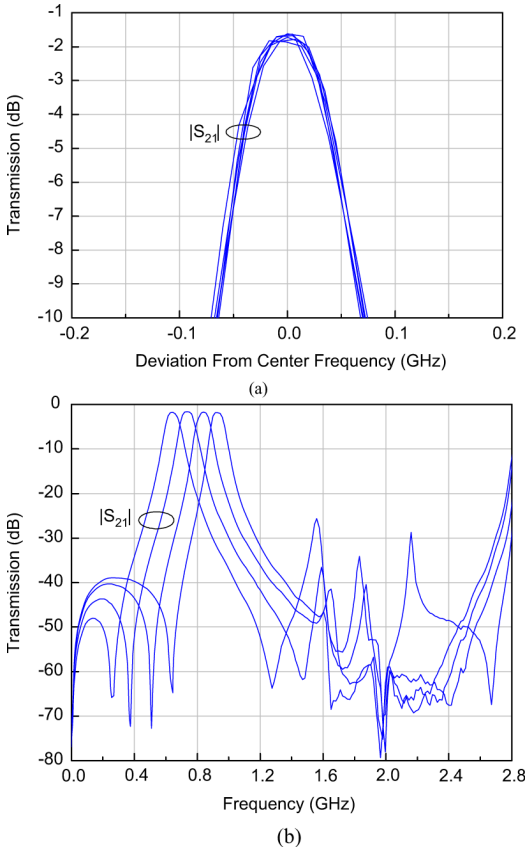

Fig. 13. Measured responses of the filter with 60-MHz bandwidth. (a) Superposition of the passband responses. (b) Wideband responses.

range, as shown in Fig. 13(a). The insertion loss ranges from 1.6 to 2.0 dB. Fig. 13(b) shows the measured wideband responses. It can be seen that the second harmonic levels are suppressed below −25 dB. The measured IIP3 is also around 13 dBm.

From the two design examples, it is observed that the second harmonic can be suppressed by simple and compact circuits and the passband performance is not affected. The absolute bandwidth and passband shape can be maintained constant over the tuning range. Moreover, the bandwidth can be controlled by changing the design parameters, indicating this topology can be used to achieve various bandwidth specifications.

V. Conclusion

In this paper, a novel method has been presented to design frequency-agile bandpass filters with constant absolute bandwidth and passband shape together with the suppressed second harmonic. Both theory and experiments have been provided, showing that Q_e and coupling coefficient variation can be controlled to fulfill the requirement of constant absolute bandwidth. The proposed resonator has a Q higher than the quarter- and half-wavelength counterparts, which, in turn, can result in low insertion loss. With the intrinsic bandpass characteristic, the compact input and output coupling networks are utilized to not only obtain desired Q_e variation, but also reduce the second harmonic. The experimental results have been presented, showing that constant absolute bandwidth and passband shape can be achieved and the second harmonic can be suppressed without degrading the passband performance. Furthermore, the absolute bandwidth can be controlled by altering the design parameters, indicating the wide applicability of this method. Transmission zeros have been generated near the passband edges, resulting in high skirt selectivity. With these features, this kind of tunable filter will be useful in multiband and wideband systems.

Acknowledgment

The authors would like to thank the editors and reviewers of this paper's manuscript for their valuable comments and suggestions, which greatly improved the quality of this paper.

References

[1] I. C. Hunter and J. D. Rhodes, "Electronically tunable microwave bandpass filters," *IEEE Trans. Microw. Theory Tech.*, vol. MTT-30, no. 9, pp. 1354–1360, Sep. 1982.

[2] A. R. Brown and G. M. Rebeiz, "A varactor-tuned RF filter," *IEEE Trans. Microw. Theory Tech.*, vol. 48, no. 7, pp. 1157–1160, Jul. 2000.

[3] B. W. Kim and S. W. Yun, "Varactor-tuned combline bandpass filter using step-impedance microstrip lines," *IEEE Trans. Microw. Theory Tech.*, vol. 52, no. 4, pp. 1279–1283, Apr. 2004.

[4] M.-S. Chung, I.-S. Kim, and S.-W. Yun, "Varactor-tuned hairpin bandpass filter with enhanced stopband performance," in *Asia–Pacific Microw. Conf.*, Dec. 2006, pp. 645–648.

[5] E. Pistono, L. Duvillaret, J.-M. Duchamp, A. Vilcot, and P. Ferrari, "Improved and compact 0.7 GHz tune-all bandpass filter," *Electron. Lett.*, vol. 43, no. 3, pp. 165–166, Feb. 2007.

[6] S.-J. Park and G. M. Rebeiz, "Low-loss two-pole tunable filters with three different predefined bandwidth characteristics," *IEEE Trans. Microw. Theory Tech.*, vol. 56, no. 5, pp. 1137–1148, May 2008.

[7] X. Y. Zhang and Q. Xue, "Novel centrally loaded resonators and their applications to bandpass filters," *IEEE Trans. Microw. Theory Tech.*, vol. 56, no. 4, pp. 913–921, Apr. 2008.

[8] M. Sanchez-Rendo, R. Gomez-Garcia, J. I. Alonso, and C. Briso-Rodriguez, "Tunable combline filter with continuous control of center frequency and bandwidth," *IEEE Trans. Microw. Theory Tech.*, vol. 53, no. 1, pp. 191–199, Jan. 2005.

[9] H. J. Park *et al.*, "A new varactor-tuned microstrip ring bandpass filter with harmonic suppression," in *Asia–Pacific Microw. Conf.*, Dec. 2000, pp. 1127–1130.

[10] J. Kim and J. Choi, "Varactor-tuned microstrip bandpass filter with wide tuning range," *Microw. Opt. Technol. Lett.*, vol. 50, no. 10, pp. 2574–2577, Oct. 2008.

[11] X.-P. Liang and Y. Zhu, "Hybrid resonator microstrip line electronically tunable filter," in *IEEE MTT-S Int. Microw. Symp. Dig.*, 2001, pp. 395–398.

[12] K. Entersari and G. M. Rebeiz, "A 12–18 GHz three-pole RF MEMS tunable filter," *IEEE Trans. Microw. Theory Tech.*, vol. 53, no. 8, pp. 2566–2571, Aug. 2005.

[13] S.-J. Park, M. A. El-Tanani, I. Reines, and G. M. Rebeiz, "Low-loss 4–6-GHz tunable filter with 3-bit high-Q orthogonal bias RF-MEMS capacitance network," *IEEE Trans. Microw. Theory Tech.*, vol. 56, no. 10, pp. 2348–2355, Oct. 2008.

[14] J. Nath, D. Ghosh, J.-P. Maria, A. I. Kingon, W. Fathelbab, P. D. Franzon, and M. B. Steer, "An electronically tunable microstrip bandpass filter using thin-film barium–strontium–titanate (BST) varactors," *IEEE Trans. Microw. Theory Tech.*, vol. 53, no. 9, pp. 2707–2712, Sep. 2005.

[15] Y.-H. Chun, J. S. Hong, P. Bao, T. J. Jackson, and M. J. Lancaster, "BST-varactor tunable dual-mode filter using variable ZC transmission line," *IEEE Microw. Wireless Compon. Lett.*, vol. 18, no. 3, pp. 167–169, Mar. 2008.

[16] S. Courreges *et al.*, "A ka-band electronically tunable ferroelectric filter," *IEEE Microw. Wireless Compon. Lett.*, vol. 19, no. 6, pp. 356–358, Jun. 2009.

[17] G. L. Matthaei, "Narrow-band, fixed-tuned, and tunable bandpass filters with zig–zag hairpin-comb resonators," *IEEE Trans. Microw. Theory Tech.*, vol. 51, no. 4, pp. 1214–1219, Apr. 2003.

[18] J. S. Hong and M. J. Lancaster, *Microwave Filter for RF/Microwave Application*. New York: Wiley, 2001.

[19] G. L. Dai, X. Y. Zhang, C. H. Chan, Q. Xue, and M. Y. Xia, "An investigation of open- and short-ended resonators and their applications to bandpass filters," *IEEE Trans. Microw. Theory Tech.*, vol. 57, no. 9, pp. 2203–2210, Sep. 2009.
[20] R. Levy, R. V. Snyder, and S. Shin, "Bandstop filters with extended upper passbands," *IEEE Trans. Microw. Theory Tech.*, vol. 54, no. 6, pp. 2503–2515, Jun. 2006.
[21] D. M. Pozar, *Microwave Engineering*, 3rd ed. New York: Wiley, 2005, pp. 307–310.

Xiu Yin Zhang (S'07–M'10) was born in Hubei Province, China. He received the B.S. degree from the Chongqing University of Posts and Telecommunications, Chongqing, China, in 2001, the M.S. degree from the South China University of Technology, Guangzhou, China, in 2006, and the Ph.D. degree from the City University of Hong Kong, Kowloon, Hong Kong, in 2009, all in electronic engineering.

From 2001 to 2003, he was with the ZTE Corporation, Shenzhen, China. From July 2006 to June 2007, he was a Research Assistant with the City University of Hong Kong. From September 2009 to February 2010, he was a Research Fellow with the City University of Hong Kong. He is currently an Associate Professor with the School of Electronic and Information Engineering, South China University of Technology, Guangzhou, China. His research interests include microwave circuits, microstrip antennas, and cognitive radios.

Dr. Zhang is the reviewer of several international journals including the IEEE MICROWAVE AND WIRELESS COMPONENTS LETTERS.

Quan Xue (M'02–SM'04) received the B.S., M.S., and Ph.D. degrees in electronic engineering from the University of Electronic Science and Technology of China (UESTC), Chengdu, China, in 1988, 1990, and 1993, respectively.

In 1993, he joined the UESTC, as a Lecturer. He became an Associate Professor in 1995 and a Professor in 1997. From October 1997 to October 1998, he was a Research Associate and then a Research Fellow with the Chinese University of Hong Kong. In 1999, he joined the City University of Hong Kong, Kowloon, Hong Kong, where he is currently an Associate Professor and the Director of the Applied Electromagnetics Laboratory. Since May 2004, he has been the Principal Technological Specialist of the State Integrated Circuit (IC) Design Base, Chengdu, Sichuan Province, China. He has authored or coauthored over 150 internationally referred papers His current research interests include antennas, smart antenna arrays, active integrated antennas, power amplifier linearization, microwave filters, millimeter-wave components and subsystems, and microwave monolithic integrated circuits (MMIC) RF integrated circuits (RFICs).

Dr. Xue is the IEEE Microwave Theory and Techniques Society (IEEE MTT-S) Regional Coordinator of IEEE Region 10. He was recognized by the UESTC as Distinguished Academic Staff for his contribution to the development of millimeter-wave components and susbsystems. He was co-supervisor of two IEEE MTT-S International Microwave Symposium (IMS) Best Student Contest papers (third place 2003 and first place 2004).

Chi Hou Chan (S'86–M'86–SM'00–F'02) received the Ph.D. degree in electrical engineering from the University of Illinois at Urbana-Champaign, in 1987.

In 1996, he joined the Department of Electronic Engineering, City University of Hong Kong, and in 1998, became Chair Professor of Electronic Engineering. From 1998 to 2009, he was the first Associate Dean and then Dean of the College of Science and Engineering, City University of Hong Kong. He is currently Acting Provost of the City University of Hong Kong. His research interests include computational electromagnetics, antennas, microwave and millimeter-wave components and systems, and RFICs.

Prof. Chan was the recipient of the 1991 National Science Foundation (NSF) Presidential Young Investigator Award and the 2004 Joint Research Fund for Hong Kong and Macau Young Scholars, National Science Fund for Distinguished Young Scholars, China Award. For teaching, he has been a four-time recipient of the Outstanding Teacher Award of the Electrical Engineering Department, City University of Hong Kong (1998–2000 and 2008). His students have also been the recipients of numerous awards including one of the 22 Special Awards of the 2003 National Challenger's Cup in China, Third Prize (2003) and First Prize (2004) of the IEEE Microwave Theory and Techniques Society (IEEE MTT-S) International Microwave Symposium (IMS) Student Paper Contests, the IEEE MTT-S Graduate Fellowship (2004–2005), Undergraduate/Pre-Graduate Scholarships (2006–2007 and 2007–2008), and the 2007 International Fulbright Science and Technology Fellowship of the U.S. Department of State.

Bin-Jie Hu (M'08) was born in Shanxi, China. He received the M.S. degree from the China Research Institute of Radiowave Propagation, Xinxiang, China, in 1991, and the Ph.D. degree from the University of Electronic Science and Technology of China, Chengdu, China, in 1997, all in electronic engineering.

From 1997 to 1999, he was a Postdoctoral Fellow with the South China University of Technology. From 2001 to 2002, he was a Visiting Scholar with the Department of Electronic Engineering, City University of Hong Kong. In 2005, he was a Visiting Professor with the Université de Nantes, Nantes, France. He is currently a Full Professor with the South China University of Technology, Guangzhou, China. His current research interests include wireless communications, cognitive radios, microwave circuits, and antennas.